Pharmacological Research 194 (2023) 106854

Contents lists available at ScienceDirect

Pharmacological Research

journal homepage: www.elsevier.com/locate/yphrs

Novel application potential of cinaciguat in the treatment of mixed hyperlipidemia through targeting PTL/NPC1L1 and alleviating intestinal microbiota dysbiosis and metabolic disorders

Ang Jia [a,1], Hongfei Jiang [b,1], Wenjing Liu [b], Pengwei Chen [c,*], Qi Xu [d,*], Renshuai Zhang [b,*], Jufeng Sun [a,*]

[a] The First Affiliated Hospital of Jinzhou Medical University, Jinzhou 121000, China
[b] The Affiliated Hospital of Qingdao University, Qingdao University, Qingdao 266071, China
[c] Hainan Key Laboratory for Research and Development of Natural Products from Li Folk Medicine, Institute of Tropical Bioscience and Biotechnology, Chinese Academy of Tropical Agricultural Sciences, Haikou 571101, China
[d] School of Pharmaceutical Sciences, Laboratory of Immunology for Environment and Health, Shandong Analysis and Test Center, Qilu University of Technology (Shandong Academy of Sciences), Jinan 250353, China

ARTICLE INFO

Keywords:
Dual inhibitors
Pancreatic triglyceride lipase
Niemann–Pick C1-like 1
Cinaciguat
Gut microbiota

Chemical compounds studied in this article:
Cinaciguat (PubChem CID: 9808022)

ABSTRACT

Mixed hyperlipidemia, characterized by high levels of triglycerides and cholesterol, is a key risk factor leading to atherosclerosis and other cardiovascular diseases. Existing clinical drugs usually only work on a single indicator, decreasing either triglyceride or cholesterol levels. Developing dual-acting agents that reduce both triglycerides and cholesterol remains a great challenge. Pancreatic triglyceride lipase (PTL) and Niemann–Pick C1-like 1 (NPC1L1) have been identified as crucial proteins in the transport of triglycerides and cholesterol. Here, cinaciguat, a known agent used in the treatment of acute decompensated heart failure, was identified as a potent dual inhibitor targeting PTL and NPC1L1. We presented in vitro evidence from surface plasmon resonance analysis that cinaciguat interacted with PTL and NPC1L1. Furthermore, cinaciguat exhibited potent PTL-inhibition activity. Fluorescence-labeled cholesterol uptake analysis and confocal imaging showed that cinaciguat effectively inhibited cholesterol uptake. *In vivo* evaluation showed that cinaciguat significantly reduced the plasma levels of triglycerides and cholesterol, and effectively alleviated high-fat diet–induced intestinal microbiota dysbiosis and metabolic disorders. These results collectively suggest that cinaciguat has the potential to be further developed for the therapy of mixed hyperlipidemia.

1. Introduction

Dyslipidemia is closely related to many cardiovascular and cerebrovascular diseases, and it is considered an especially important risk factor for atherosclerotic cardiovascular diseases [1]. Patients with mixed hyperlipidemia often show elevated cholesterol and triglyceride levels at the same time, which is more dangerous and difficult to treat than the elevation of cholesterol or triglyceride levels alone [2]. Existing clinical agents usually only reduce a single indicator (triglycerides or cholesterol), and they have limited efficacy in the treatment of mixed hyperlipidemia [3,4]. For example, statins reduce cholesterol, while fibrates lower triglyceride levels [5]. A combination of drugs can reduce triglyceride and cholesterol levels at the same time; however, liver function injury may easily occur due to pharmacokinetic interactions, which leads to poor drug tolerance during clinical treatment. For example, the combination of triglyceride-lowering fibrates and

Abbreviations: PTL, pancreatic triglyceride lipase; NPC1L1, Niemann-Pick C1-like 1; SPR, surface plasmon resonance; HFD, high-fat diet; 4-MUO, 4-methylumbelliferyl oleate; NBD-cholesterol, 22-(N-(7-Nitrobenz-2-Oxa-1,3-Diazol-4-yl) Amino)– 23,24-Bisnor-5-Cholen-3β-Ol; EDC, N-ethyl-N′-(dimethylaminopropyl)-carbodiimide; NHS, N-hydroxysuccinimide; MD, molecular dynamics; RMSD, root-mean-squared deviation; 4-MU, 4-methylumbelliferone; RU, response units; HDL-C, high density lipoprotein cholesterol; LDL-C, low density lipoprotein cholesterol; H&E, hematoxylin and eosin; OTUs, operational taxonomic units; PCoA, principal coordinates; F/B, Firmicutes/Bacteroidetes; PCA, principal component analysis; PLS-DA, partial least squares discrimination analysis.

* Corresponding authors.
E-mail addresses: chenpengwei@itbb.org.cn (P. Chen), xuqi8270@sina.com (Q. Xu), zhangrenshuai@qdu.edu.cn (R. Zhang), jzleo0810@126.com (J. Sun).
[1] These authors contributed equally to this work

https://doi.org/10.1016/j.phrs.2023.106854
Received 12 May 2023; Received in revised form 9 July 2023; Accepted 14 July 2023
Available online 17 July 2023

cholesterol-lowering statins may lead to severe myolysis, liver injury, acute kidney failure, and other toxic side effects [2]. Thus, the development of bifunctional agents that can effectively reduce triglyceride and cholesterol levels simultaneously is an effective strategy for the treatment of mixed hyperlipidemia to avoid the toxic side effects caused by drug combination.

Pancreatic triglyceride lipase (PTL) and Niemann–Pick C1-like 1 (NPC1L1) have been identified as attractive therapeutic targets for inhibiting the uptake of triglycerides and cholesterol, respectively [6,7]. The physiological roles of PTL and NPC1L1 are depicted in Fig. 1. PTL is the principal lipolytic enzyme synthesized and secreted by the pancreas, which removes fatty acids from the α and α' position of triglycerides to yield monoglycerides and long-chain fatty acids [8]. The hydrolyzed products of triglycerides are taken up by the small intestinal epithelial cells through passive diffusion, and they are then used to resynthesize triglycerides in vivo. PTL is responsible for the hydrolysis of 50–70% of total dietary fats; thus, it plays key roles in regulating triglyceride levels [6]. PTL inhibitors have been extensively studied for decreasing triglyceride levels by reducing dietary sources of triglycerides [9]. NPC1L1 is a specific transporter for cholesterol that is abundantly expressed in the small intestine of humans, and it is responsible for transporting intestinal cholesterol into the body [10]. Intestinal cholesterol absorption is an important source of plasma cholesterol. Inhibition of the intestinal cholesterol absorption is an effective strategy to reduce plasma cholesterol, especially for patients who are intolerant to high-dose statins or those who have not achieved the desired outcome after statin therapy [3]. Therefore, NPC1L1 is considered an important target for the development of cholesterol-lowering drugs. Thus far, some molecules have shown NPC1L1-inhibiting activity; however, only a few agents among these NPC1L1 inhibitors have been verified to reduce cholesterol in vivo [11].

Considering the key roles of PTL and NPC1L1 in the absorption of triglycerides and cholesterol, the design of PTL/NPC1L1 dual inhibitors is considered an effective strategy to achieve the simultaneous reduction of triglycerides and cholesterol. According to our previous study, dual inhibitors targeting PTL and NPC1L1 can inhibit the hydrolysis of triglycerides and the uptake of cholesterol in cell models [12]. However, the PTL/NPC1L1 dual inhibitors based on β-lactone derivatives in our previous study have not demonstrated lipid-lowering activity in vivo. Since then, efforts to screen dual inhibitors with in vivo activity have been ongoing in our group. High-throughput virtual screening is an ideal strategy to uncover biologically active compounds from large-scale collections of chemical compound libraries [13]. The crystal structure of PTL was reported in 1995 [14], while the crystal structure of NPC1L1 was reported by three different research groups in 2020 and 2021 [15–17]. Thus, we attempted to obtain novel and potent PTL/NPC1L1 dual inhibitors through high-throughput virtual screening of commercially available compound libraries with diverse molecules.

The gut microbiota plays crucial roles in metabolic disorders through interacting with the host by the production of a diverse reservoir of metabolites. Growing evidence suggests that dyslipidemia is accompanied by alterations in the gut microbiota and gut microbiota–derived metabolites [18,19]. In addition, a large number of studies have shown

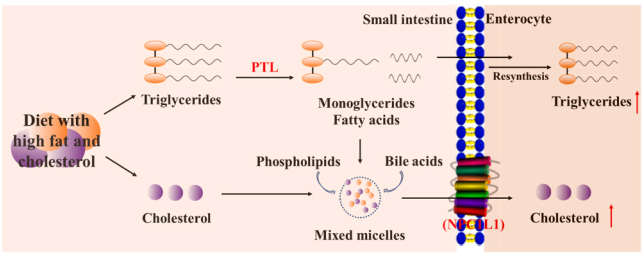

Fig. 1. Physiological roles of PTL and NPC1L1 in the absorption of triglycerides and cholesterol.

that exogenous compounds can affect the gut microbiota and gut microbiota–derived metabolites, and some of these compounds have been demonstrated to attenuate dyslipidemia via modulating the gut microbiota and gut microbiota–derived metabolites [20–22]. PTL and NPC1L1 play key roles in the gut; however, the effects of PTL/NPC1L1 dual inhibitors on the gut microbiota and its metabolites are unclear. Therefore, to unravel the potential lipid-lowering mechanisms of PTL/NPC1L1 dual inhibitors, the effects of targeted compounds on the gut microbiota and metabolites should also be explored.

In the present study, commercially available compound libraries containing more than 20,000 small molecules were first screened utilizing high-throughput virtual screening strategies based on the catalytic active site of PTL and the cholesterol-binding site of NPC1L1 in order to identify efficient agents against mixed hyperlipidemia. Then, surface plasmon resonance (SPR) was used to further narrow down the screening range of the potential PTL/NPC1L1 dual inhibitors by analyzing the interactions between the inhibitors and PTL or NPC1L1. After assaying the inhibition activity of the potential active molecules against PTL and NPC1L1 by fluorescence-based biochemical analysis, cinaciguat was identified as the target molecule for further evaluation. High-fat and cholesterol–induced C57BL/6 J mice were used to evaluate the in vivo activity of cinaciguat. Moreover, the effects of cinaciguat on the intestinal microbiota and metabolism were also carefully investigated by 16 S sequencing and untargeted metabolomics analysis.

2. Materials and methods

2.1. Reagents and materials

4-methylumbelliferyl oleate (4-MUO), 22-(N-(7-Nitrobenz-2-Oxa-1,3-Diazol-4-yl) Amino)− 23,24-Bisnor-5-Cholen-3β-Ol (NBD-cholesterol), and filipin were purchased from J&K Scientific. N-ethyl-N′-(dimethylaminopropyl)-carbodiimide (EDC), CM5 sensor chips, PBS-P buffer, N-hydroxysuccinimide (NHS), and 1.0 M ethanolamine-HCl, pH 8.5 were purchased from GE Healthcare (Mississauga, ON, Canada). Age-matched (8 weeks old, 20–25 g) male C57BL/6 J mice were purchased from Beijing Vital River Laboratory Animal Technology Company (Beijing, China). All antibodies were purchased from Proteintech (Wuhan, Hubei, China).

2.2. Molecular docking and molecular dynamics (MD) studies

Docking simulations were carried out by means of the SYBYL-X 2.0 software. All the ligand molecular were drawn using the standard parameters of SYBYL-X, then their geometric conformations were energy minimized employing the Tripos force field for 1000 steps and Gasteiger-Huckel charges were calculated. Protein receptor was prepared using the standard way: selecting substructures; removing water molecules; adding hydrogens; setting atom types (AMBER7 FF99); adding charges (Gasteiger-Huckel); staging minimization (min energy change 0.05, simplex threshold 1000). The generation of docking pocket was selected based on the "ligand mode". The H-bonds were shown using dotted line. Pymol was used as a viewer for interaction between ligands and protein receptor.

MD simulations were performed on PTL (PDB code: 1LPB) and NPC1L1 (PDB code: 6V3F) in complex with cinaciguat, respectively by using GROMACS (gmx version 5.1.4 and gmx_mpi 2019.4). GAFF and FF99SB force field were employed for the ligand and the receptors, respectively. Prior to the MD simulations, the complex was solvated into a truncated octahedral TIP3P water box and neutralized by using Na^+. The distance of the solute from the edge of the periodic box is 15 Å. Then, it was minimized to remove unfavorable vander Waals interactions. During minimization, the whole system was subjected to 50000 steps of steepest descent minimization. The cutoff of the non-bonded interactions was set to 12 Å for the energy minimization process. After minimization, MD was performed. First, the whole system

was gradually heated to 300 K in 100 ps in the NVT ensemble. Then the system was equilibrated in the NPT ensemble where the temperature and pressure were kept at 300 K and 1 atm respectively. Finally, a 50-ns molecular dynamics process was carried out. The root-mean-squared deviation (RMSD) of the protein Cα atoms was calculated to monitor the global and local conformational flexibility. The H-bond was recorded when the donor–acceptor distance was less than 3.5 Å and the donor–hydrogen–acceptor angle was larger than 120°. The binding free energy (Δ Gbind) between the receptor and the ligand in each system was calculated by the MM/GBSA methodology. The trajectories of each system were used for the binding free energy calculation with the MMPBSA.py module in AMBER16.

2.3. PTL inhibitory activity assay

The inhibitory activity of cinaciguat against PTL was investigated using 4-MUO as a substrate, according to the previous method [23]. Cinaciguat solution with different concentrations (25 μl) and PTL solution (25 μl, 1 mg/ml) were added into a black bottom 96-well plate. After pre-incubation at 37 °C for 10 min, the reaction was initiated by addition of 4-MUO (50 μl, 1 mM). After incubation at 37 °C for 20 min, the reaction was stopped by adding 100 μl of 0.1 M citrate buffer solution (pH = 4.2). The fluorescence signal of 4-methylumbelliferone (4-MU) released by PTL was measured with a fluorometrical microplate reader at an excitation wavelength of 355 nm and an emission wavelength of 460 nm. The PTL inhibitory activity of cinaciguat was evaluated by the IC_{50} values.

2.4. Cholesterol uptake assay

The cholesterol uptake assay was carried based on the method that we published earlier [24]. The NBD-cholesterol was utilized to trace cholesterol absorption in HepG2 cells. Cinaciguat and NBD-cholesterol were formulated using 0.5 mM taurine sodium salt (Beyotime, Shanghai, China). Before checking cholesterol absorption, the culture medium with 10% FBS was replaced with the medium containing the LPDS, and followed incubated 24 h. Cells were then washed 3 times with PBS buffer, incubated with drugs for 4 h, and then NBD-cholesterol for 1 h. Cells were washed three times in PBS to remove NBD-cholesterol that was not ingested into cells, and then the fluorescence was measured at excitation and emission wavelengths of λex = 485 nm and λem = 535 nm, respectively.

2.5. Filipin staining

A fresh 5 mg/ml stock solution of filipin was prepared according our previous study [24]. HepG2 cells were cultured in confocal culture chambers at different drug concentrations for 2 h. After being washed three times with PBS, cells were fixed by adding 4% formaldehyde. Cells were washed twice with PBS and stained with 50 μg/ml filipin in the dark for 30 min at room temperature followed by three washes with PBS. Images were captured using a Nikon confocal microscope (Nikon Instruments, Tokyo, Japan). Red pseudocolor was assigned to show the filipin signal.

2.6. SPR studies

The SPR study was based on the experimental method we reported earlier [12]. In briefly, SPR interaction analysis was carried out using Biacore T200 from GE Healthcare Life Sciences. PTL and NPC1L1 (both final concentration 50 μg/ml) were dissolved in 10 mM sodium acetate buffer (pH 4.5) and immobilized to a CM5 chip. The surface of flow cell was activated for 7 min using a 1:1 mixture of 100 mM EDC and 100 mM NHS in the flow rate of 10 μl/min, and subsequently the corresponding proteins was injected over the surface for 7 min using a Time and Flow method (final immobilization level: 8000–12000 response units (RU)). Excess reactive esters on the sensor chip surface were blocked with 1 M ethanolamine (pH 8.5) for 7 min. Flow cell used for reference was activated and blocked as described above, but remained uncoupled. Binding was usually reported in RU, which was defined as the response obtained from the flow cell containing the immobilized receptor minus the response obtained from the reference flow cell.

2.7. Animal studies

All experimental procedures involving animals were approved by the Animal Care and Use Committee of Qingdao University (NO. QDU-AEC-2022482). After acclimation for a week in the laboratory environment with 25 ± 2 °C temperature, and 12/12 h light/dark cycle, the mice were randomly distributed in six groups (each with n = 8): the control group, HFD (high-fat diet) model group, the orlistat (40 mg/kg/day) treated group, ezetimibe (10 mg/kg/day) treated group, high doses cinaciguat treated group (100 mg/kg/day), and low doses cinaciguat treated group (10 mg/kg/day). The dose of cinaciguat was set according to the inhibitory activity of cinaciguat against PTL and NPC1L1. The control group was fed with normal rat chow, while all the other groups were fed with HFD which was made by addition of 10% cholesterol and 20% lard to the normal rat chow. The mice were administrated with distilled water or their corresponding drugs by oral gavages once every morning for 8 weeks. During the whole experiment period, the body weight of individual mice was recorded weekly. At the end of experimental period, all mice were sacrificed followed by the collection of blood and tissues for further analysis. In briefly, the serum was collected by centrifuging whole blood (3000 rpm, 10 min), and triglycerides, total cholesterol, high density lipoprotein cholesterol (HDL-C) and low density lipoprotein cholesterol (LDL-C) levels were determined by standardized enzymatic procedures using the Nanjing KeyGEN Biotec's kits (Nanjing, China), the liver tissue fixed in 4% paraformaldehyde for histological analysis, the small intestine tissue was frozen in liquid nitrogen for protein extraction, and feces from the rectum were frozen in liquid nitrogen immediately and then were stored in the − 80 °C. Five samples of every group were selected randomly for gut microbiota and metabolomic analysis.

2.8. Histological Analysis

For histological analysis, the fixed liver tissues were embedded in paraffin and cut into 3 μm thick sections. Then, the sections were stained with hematoxylin and eosin (H&E) to evaluate liver injury. Frozen liver tissues were cut into 5 μm sections and stained with oil red O to analyze hepatic lipid accumulation.

2.9. Western blot analysis

The analysis of NPC1L1 expression in small intestine tissue was performed as reported previously [12]. In briefly, total proteins from the small intestine tissue were extracted with RIPA solution. The contents of protein solutions were detected using the bicinchoninic acid protein assay kit. Proteins from the samples were electrophoresed on SDS polyacrylamide gels and then transferred onto PVDF membranes. Membranes were blocked in 5% non-fat milk and then incubated with primary antibodies overnight at 4 ℃, followed by incubation with secondary antibodies for 1 h at room temperature. Membranes were washed three times with TBST for 5 min each time. Finally, the chemiluminescence method was employed to detect the signals using Pierce™ ECL Western Blotting Substrate (Thermo Scientific, Waltham, MA, USA) and protein bands were detected by autoradiography and the intensities were analyzed by Image J public domain software from the National Institutes of Health (Bethesda, MD, USA). The antibodies for GAPDH and NPC1L1 were purchased from BOSTER (China).

2.10. Analysis of gut microbiota

The composition of the gut microbiota in feces was analyzed using 16 S rRNA sequencing that was performed according to a previous study [25]. In briefly, total genomic DNA samples were extracted using the OMEGA Soil DNA Kit (M5635–02) (Omega Bio-Tek, Norcross, GA, USA), following the manufacturer's instructions, and stored at − 20 °C prior to further analysis. The quantity and quality of extracted DNAs were measured using a NanoDrop NC2000 spectrophotometer (Thermo Fisher Scientific, Waltham, MA, USA) and agarose gel electrophoresis, respectively. PCR amplification of the bacterial 16 S rRNA genes V3–V4 region was performed using the forward primer 338 F(5′-ACTCCTACGGGAGGCAGCA-3′) andthereverse primer806 R (5′-GGACTACHVGGGTWTCTAAT-3′). PCR amplicons were purified with Vazyme VAHTSTM DNA Clean Beads (Vazyme, Nanjing, China) and quantified using the Quant-iT PicoGreen dsDNA Assay Kit (Invitrogen, Carlsbad, CA, USA). After the individual quantification step, amplicons were pooled in equal amounts, and pair-end 2250 bp sequencing was performed using the Illlumina MiSeq platform with MiSeq Reagent Kit v3 at Shanghai Personal Biotechnology Co., Ltd (Shanghai, China). Raw data were merged and filtered to obtain the clean data. Operational taxonomic unit (OTU) clustering was performed using UPARSE software (sequence similarity was set at 97%) based on these clean data. Then the OTUs were annotated to taxonomic information followed by the α-diversity, β-diversity, and community composition analysis using R software.

2.11. Metabolomic analysis

Metabolites were extracted using 1 ml precooled mixtures of methanol, acetonitrile and water (v/v/v, 2:2:1) and then placed for 1 h ultrasonic shaking in ice baths. Subsequently, the mixture was placed at − 20 °C for 1 h and centrifuged at 14,000 g for 20 min at 4 °C. The supernatants were recovered and concentrated to dryness in vacuum. The metabolome profile was measured using UPLC-ESI-Q-Orbitrap-MS system (UHPLC, Shimadzu Nexera X2 LC-30AD, Shimadzu, Japan) coupled with Q-Exactive Plus (Thermo Scientific, San Jose, USA). Quality control (QC) samples were prepared by pooling aliquots of all samples that were representative of the samples under analysis, and used for data normalization. Blank samples (75%ACN in water) and QC samples were injected every six samples during acquisition. The raw MS data were converted to MzXML files using ProteoWizard MSConvert and processed using XCMS for feature detection, retention time correction and alignment. The metabolites were identified by accuracy mass (< 25 ppm) and MS/MS data which were matched with a standards database.

2.12. Statistical Analysis

All data in this study were presented as mean ± standard error of the mean (SEM) values. Statistical comparisons were analyzed by one-way analysis of variance (ANOVA) followed by Fisher's least significant difference (LSD) test (SPSS 19.0). A difference of $^{*}P < 0.05$, $^{**}P < 0.01$, and $^{***}P < 0.001$ was considered statistically significant. Statistical evaluations were performed using GraphPad Prism 8.0 (San Diego, CA, USA).

3. Results

3.1. Screening of PTL/NPC1L1 dual inhibitors

We selected the crystal structures of PTL (PDB code: 1LPB) and NPC1L1 (PDB code: 6V3F) as our binding template, which exhibited clear electron densities and high resolution of 2.4 and 3.7 (Å), respectively. In addition, the crystal structure of PTL (PDB: 1LPB) showed open conformation in the catalytic active site, which was more conducive to substrate binding than PTL with closed conformation (e.g., PDB: 1N8S). The structure of NPC1L1 used in our virtual screening was also open-state, displaying the cholesterol-binding cavity open for cholesterol loading. Moreover, the binding pockets formed by the catalytic active site of PTL and the cholesterol-binding site of NPC1L1 were very similar: narrow and long (Fig. S1). A flowchart of the multistep screening strategy for PTL/NPC1L1 dual inhibitors is shown in Fig. 2A. The proteins were prepared by using Protein Preparation Workflow of the software package by hydrogen addition and energy minimization. Then, all of the compounds from a commercially available small library were energy-minimized and docked into the binding pocket of PTL. Then, 200 top-ranked compounds with the highest total binding scores were selected for further consideration. Next, they were docked into NPC1L1, and 30 top-ranked compounds were selected for further SPR assay. Following the workflow system, we finally identified 11 compounds that showed binding potential to both PTL and NPC1L1. Structures and binding sensorgram of these compounds are displayed in Figs. S2–S4. Then, we evaluated the inhibitory activities of the 11 compounds against PTL and NPC1L1 using 4-MUO and NBD-cholesterol methods, respectively, as shown in Table S1. Most of the compounds only displayed the inhibitory activity against NPC1L1-mediated cholesterol uptake, including compounds 5, 6, 9, and 10, which have been reported in our previous studies [24,26–28]. Compound 11, also known as cinaciguat, showed moderate inhibitory activity against PTL with IC_{50} of 3.7 μM (Table S1, Fig. 2B). Although the activity of cinaciguat was weaker than that of orlistat (IC_{50} < 10.0 nM), an FDA-approved PTL inhibitor, the activity of cinaciguat was still considered desirable because cinaciguat is a noncovalent inhibitor, whereas orlistat is a covalent inhibitor [29]. In addition, cinaciguat demonstrated higher inhibitory activity than ezetimibe, an FDA-approved NPC1L1 inhibitor, at 100 μM concentration (Table S1, Fig. 2C). Cinaciguat is a soluble guanylate cyclase activator, and it has shown a wide range of pharmacological activities against heart disease, nephropathy, and osteoporosis [30–32]. Further, Zhao et al. demonstrated that cinaciguat showed lipid-lowering activity in diabetic mice [33]. However, the lipid-lowering mechanism of cinaciguat remains unclear, and its effectiveness has not been studied in hyperlipidemia models. The study on the lipid-lowering activity of cinaciguat could further expand its clinical application potential. Thus, cinaciguat was identified as the target molecule for further study. Studies of cinaciguat at molecular, cellular, and animal levels are described below.

3.2. Molecule docking and MD studies

As part of the high-throughput virtual screening, molecular docking simulation was performed to assay the binding model of cinaciguat with PTL and NPC1L1. The results of docking are displayed in Fig. 3. The long and narrow molecular structure of cinaciguat only occupied the cavity of the binding site of PTL (Fig. 3A) and NPC1L1 (Fig. 3B). Meanwhile, the carboxyl group on the benzene ring played key roles in the binding, forming hydrogen bonding interaction with Ser152 at the PTL catalytic site and Ser187 at the NPC1L1 cholesterol-binding site. The *Total Score* (an index indicating binding affinity in molecular docking using the SYBYL-X 2.0 software) were 6.2 (cinaciguat and PTL) and 7.7 (cinaciguat and NPC1L1) respectively. In addition, the binding energy of cinaciguat with PTL or NPC1L1 were − 25.9 kcal/mol and − 23.7 kcal/mol in MD simulations, respectively. Moreover, the stability of these hydrogen bonds was evaluated by calculating the evolution of distances between the H-bond interacting atoms in 50-ns MD simulations. The results suggested that hydrogen bonds between receptors (PTL or NPC1L1) and cinaciguat were always present throughout the MD simulation (Fig. S5). The distance between Ser152 and cinaciguat in the PTL/cinaciguat complex showed almost no fluctuation during the whole MD process. Although the distances between Ser187 and cinaciguat showed slight fluctuation at 20–30 ns, the distances reached equalization and remained constant in the following 20 ns. Furthermore, RMSD was used to assess the distance between two aligned objects, as shown in

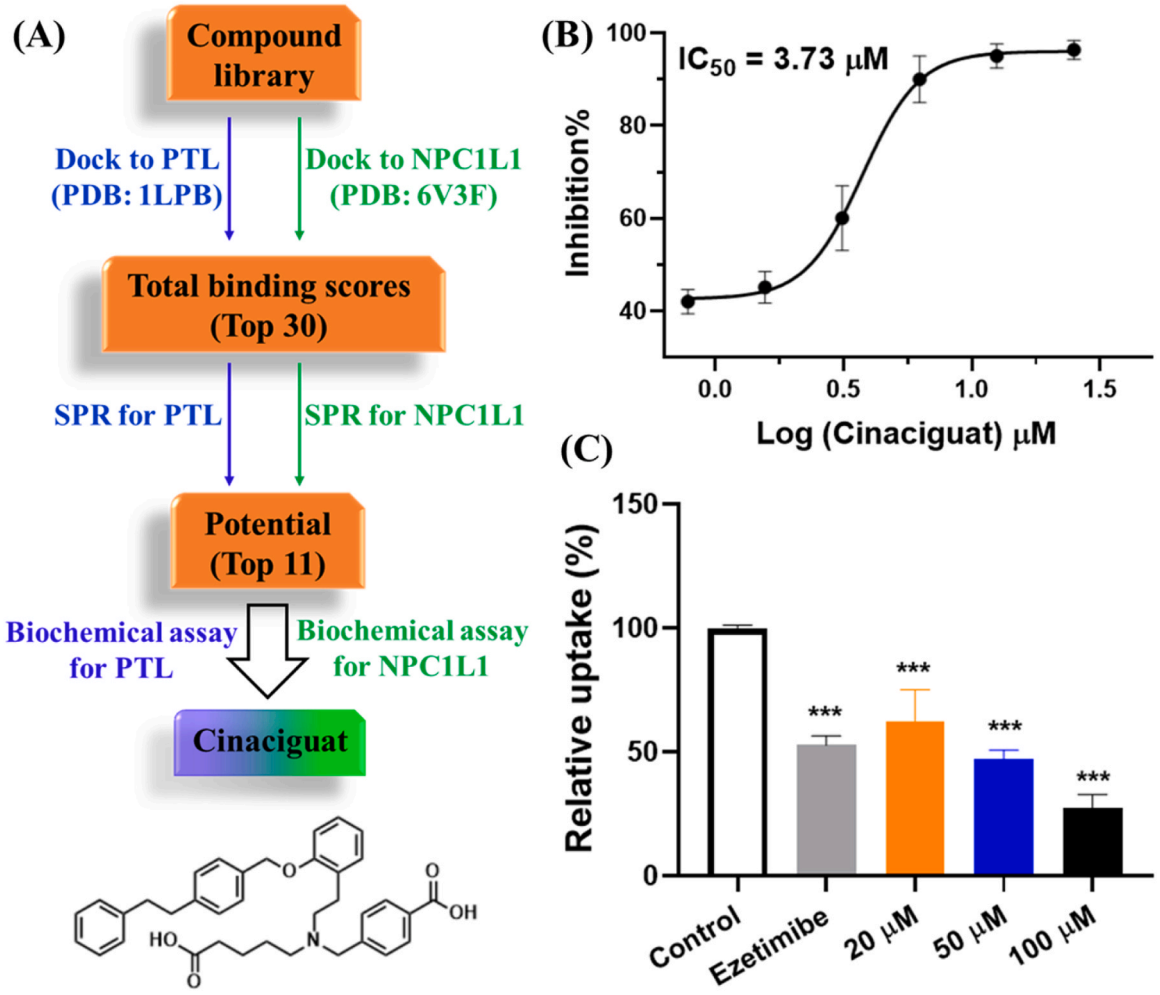

Fig. 2. Screening of PTL/NPC1L1 dual inhibitors. (A) Flowchart of the multistep screening strategy for PTL/NPC1L1 dual inhibitors. (B) Inhibition activity assay of cinaciguat against PTL. The IC_{50} was calculated from the fitted curve. (C) Assay of the effect of cinaciguat (20, 50, and 100 μM) on the uptake of NBD-cholesterol in HepG2 cells. Positive control: ezetimibe in 100 μM. * ** $P < 0.001$ compared with the control.

Figs. 3C and 3D. The conformation of cinaciguat bound to PTL always remained stable in the total MD process. After 60-ns simulation, the conformation of cinaciguat bound to NPC1L1 began to remain stable. For PTL and NPC1L1, there was no significant difference between the superposed images before and after MD simulation (Fig. S6), which also demonstrated the stability of protein conformation during dynamic simulation. All of the above observations suggested that the interaction between cinaciguat and PTL (or NPC1L1) was potent and stable, which may be the key, at least in part, for the inhibitory effect of cinaciguat.

3.3. Interaction of cinaciguat with PTL and NPC1L1 by SPR assay

The interaction between cinaciguat and PTL (or NPC1L1) was also studied by SPR, which is a powerful tool in drug discovery that is used to characterize the interaction between target proteins and drugs. The SPR traces presented in Fig. 4A indicate that cinaciguat is able to interact with PTL in a concentration-dependent manner. Similar results can be observed in the binding between cinaciguat and NPC1L1 (Fig. 4B).

3.4. Cinaciguat is a competitive inhibitor of PTL and NPC1L1

Because the binding cavity used in the high-throughput screening was the catalytic active site of PTL and the substrate-binding site of NPC1L1, theoretically, targeted molecules obtained by this screening method should be competitive inhibitors. To further confirm this hypothesis, the inhibition kinetics of cinaciguat against PTL-mediated 4-MUO hydrolysis and NPC1L1-mediated cholesterol uptake were measured by adding various concentrations of cinaciguat into the incubation systems with different concentrations of the substrates (4-MUO or NBD-cholesterol). As illustrated in Fig. 5, the Lineweaver–Burk plots indicate that cinaciguat is able to decrease the reaction rates of PTL-mediated 4-MUO hydrolysis (Fig. 5A), and inhibit NPC1L1-mediated cholesterol uptake (Fig. 5B) as a competitive inhibitor. The results are consistent with the extrapolations from the virtual screening.

3.5. Cinaciguat inhibits NPC1L1-mediated cholesterol uptake in Filipin staining assay

Filipin staining experiments have been used by Ge et al. to examine NPC1L1-mediated cholesterol uptake [34]. According to our previous studies, HepG2 cells highly express NPC1L1, so they are suitable to evaluate the inhibitory activity of compounds against NPC1L1-mediated cholesterol absorption [24,28]. In the current study, we stained HepG2 cells with filipin, a sterol-binding fluorescent dye, to indicate the amount of cellular cholesterol after cinaciguat treatment. The treatment process for HepG2 cells is shown in Fig. 6 A. First, HepG2 cells were cultured in a cholesterol-depleting medium for 60 min to deplete cholesterol in the cells, and then treated with cinaciguat for 60 min. Finally, a cholesterol-replenishing medium was added. Confocal images were obtained at − 60 min and 60 min. Ezetimibe, an FDA-approved

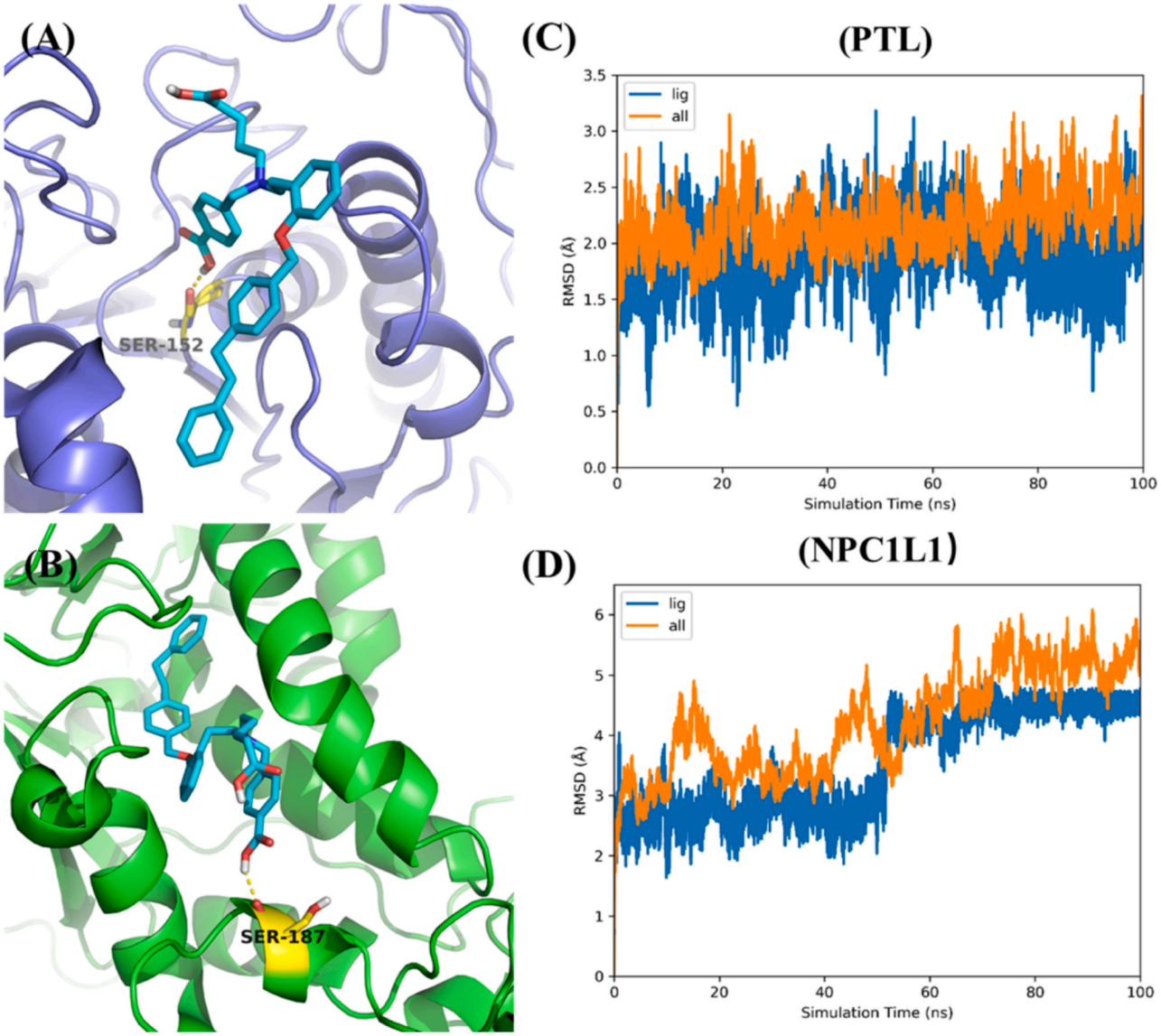

Fig. 3. Binding modes of cinaciguat to PTL (PDB: 1LPB) (A) and NPC1L1 (PDB: 6V3F) (B). Cinaciguat is shown in color by element (carbon in cyan). The H-bonds are displayed using yellow dashed lines. The key amino acid residues are shown in color by element (carbon in yellow). Root-mean-squared deviation (RMSD) of cinaciguat binding to PTL (C) and NPC1L1 (D) in MD simulation.

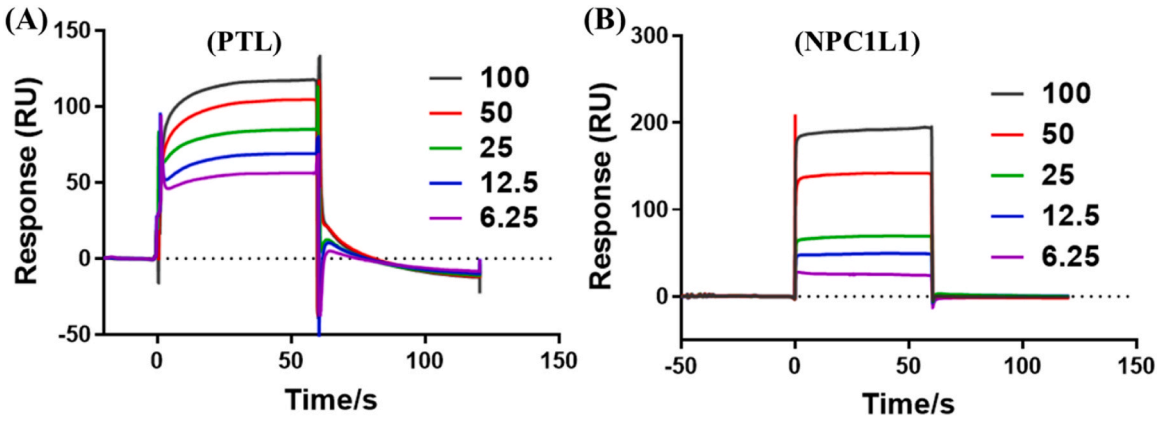

Fig. 4. Binding sensorgram for cinaciguat interaction with immobilized PTL (A) and NPC1L1 (B). The concentration was 6.25, 12.5, 25, 50, and 100 μM.

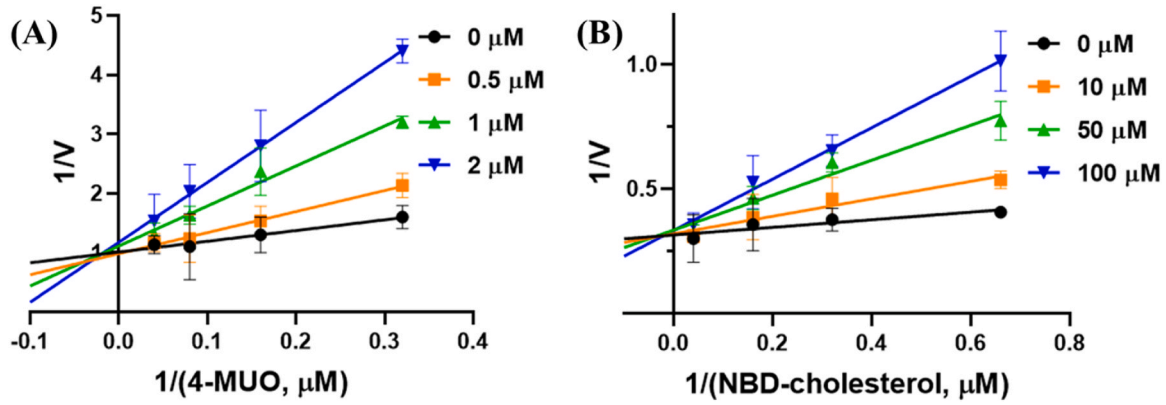

Fig. 5. Lineweaver–Burk plots of cinaciguat against PTL (A) and NPC1L1 (B) at different concentrations. Each value represents the mean ± S.D. (n = 3 independent experiments).

NPC1L1 inhibitor, was used as the positive control. As shown in Fig. 6B, cholesterol was barely observed in HepG2 cells after incubation in the cholesterol-depleting medium for 60 min. However, after readding the cholesterol-replenishing medium for 60 min, cholesterol in HepG2 cells significantly increased. Interestingly, cinaciguat inhibited the fluorescence recovery of stained cholesterol, indicating that cinaciguat can inhibit the transport of cholesterol from the medium into the cells. Fluorescence quantification displayed in Fig. 6 C reveals consistent results.

3.6. Evaluation of hypolipidemic activity in vivo

The abovementioned results encouraged us to further investigate the hypolipidemic activity of cinaciguat in vivo. HFD was used to induce mixed hyperlipidemia. The body weight of the mice was recorded weekly. Triglycerides, total cholesterol, HDL-C, and LDL-C were measured at the end of the experiment. In addition, the effect of cinaciguat on the expression of NPC1L1 in the small intestine was detected by western blot. As shown in Fig. 7 A, HFD-fed mice showed a significant increase in body weight compared with the control group. The observed final body weight was significantly lower in the high-dose cinaciguat (Cinaiguat-H, 100 mg/kg/day)–treated group than in the HFD group (no drug treatment). In addition, high-dose cinaciguat treatment significantly decreased triglyceride and total cholesterol levels, which were similar to the positive control orlisitat and ezetimibe, respectively (Fig. 7B). Furthermore, compared with the HFD group, the obviously increased HDL-C level and significantly decreased LDL-C level were observed in the Cinaiguat-H group (Fig. 7 C). All of these data indicate that cinaciguat can effectively reduce blood lipids. Moreover, HFD induced high expression of NPC1L1 in the small intestine, which could further promote intestinal cholesterol absorption, whereas cinaciguat treatment reduced the change in NPC1L1 expression (Fig. 7D). HFD usually induces hepatic steatosis, which may be improved by lowering blood lipids. Thus, the improvement effect on hepatic steatosis after cinaciguat treatment was evaluated by H&E and oil red-O staining. As shown in Fig. 8, HFD dramatically promoted lipid vacuoles and lipid droplet accumulation in the liver, causing hepatic steatosis, while cinaciguat treatment significantly attenuated these hepatic disorders.

3.7. Gut microbiome composition is modulated by cinaciguat

To comprehensively investigate the effect of cinaciguat on the intestinal health in mixed-hyperlipidemia mice, the gut microbiota composition was explored by 16 S sequencing analysis. The Venn

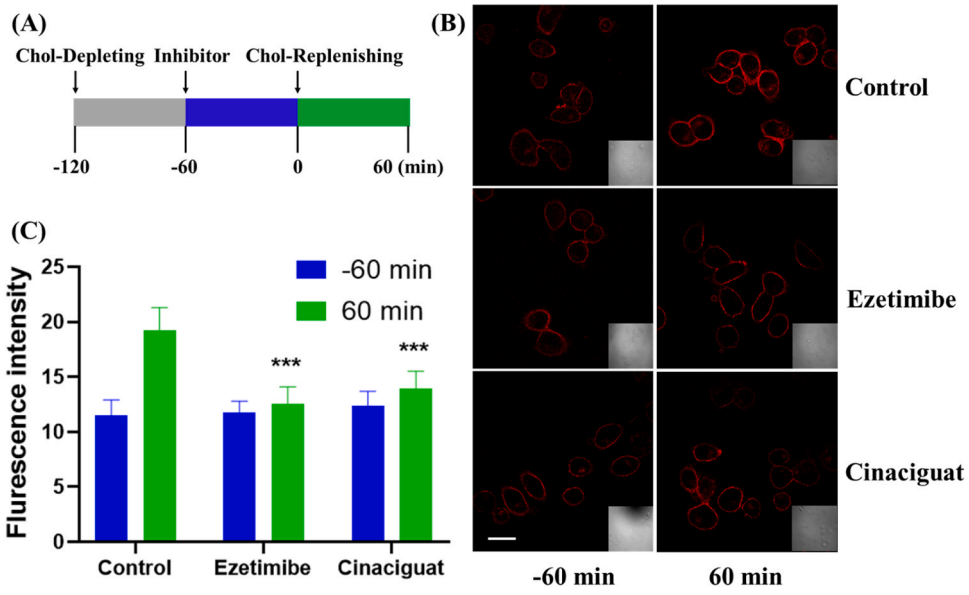

Fig. 6. (A) Diagram showing the procedure used to treat the cells. Chol: cholesterol. (B) Image of HepG2 cells that were treated as shown in (A); Scale bar = 20 μm. (C) Quantification of intracellular cholesterol of HepG2 cells. Error bars represent standard deviations. * ** $P < 0.001$ compared with the control (60 min).

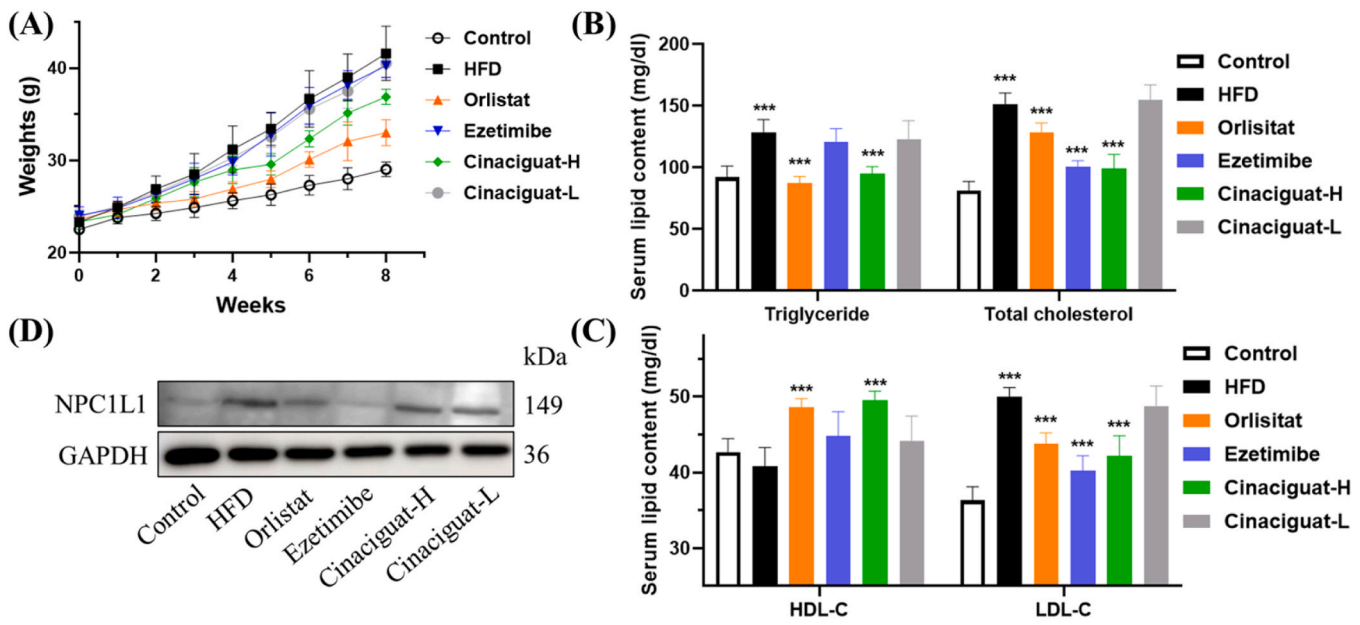

Fig. 7. (A) Effect of cinaciguat on the body weight. Serum concentrations of triglycerides and total cholesterol (B), HDL-C, and LDL-C (C). (D) Western blot analysis of NPC1L1 protein expression in the small intestine tissue with GAPDH as an internal control. HDL-C: high-density lipoprotein–cholesterol, LDL-C: low-density lipoprotein–cholesterol. * ** $P < 0.001$ HFD compared with the control, or other groups compared with HFD.

diagram (Fig. 9A) revealed 1439 OTUs in the control group, 1692 OTUs in the HFD group (HFD group without cinaciguat treatment), and 2917 OTUs in the Treat group (cinaciguat group). The cinaciguat group showed a higher number of identical of OTUs with the Control group than with the HFD group (433 vs. 425). In α-diversity analysis, HFD consumption led to a significant decrease in Shannon (Fig. S7A) and Simpson indexes (Fig. S7B) compared with the control group. Although there was also a decrease in the Chao1 and Observed species index in the Treat group, the reduction was not significant compared with the control group (Fig. 9B, C). These results suggested that HFD exposure decreased the richness and diversity in the bacterial communities, while cinaciguat treatment partially reversed these changes. In addition, the principal coordinates (PCoA) score plot of β-diversity analysis, based on unweighted and weighted UniFrac, revealed that the HFD group distinctly formed separate clusters from the Control group; however, the Treat group did not show distinct clustering from the HFD group (Fig. 9D, S7C). Further multivariate pairwise comparisons revealed the significant differences between the Control group and the HFD group, and between the Control group and the Treat group (Fig. S7D). The results of the taxonomic analysis suggested that the gut microbiota in all of the samples was dominated by four major phyla, namely, Firmicutes, Bacteroidetes, Proteobacteria, and Verrucomicrobiota (Fig. 9E). In the HFD group, Firmicutes increased and Bacteroidetes decreased, which caused an increase in the Firmicutes/Bacteroidetes (F/B) ratio (2.9) compared with that in the Control group (0.91). F/B is considered an indicator associated with metabolic disorders [20]. Notably, cinaciguat treatment slightly decreased the F/B ratio (2.6). The order-level analysis revealed relatively lower abundance of *Bacteroidales* and relatively higher abundance of *Clostridiales* in the HFD group compared with the Control group, whereas these changes were weakened in the Treat group

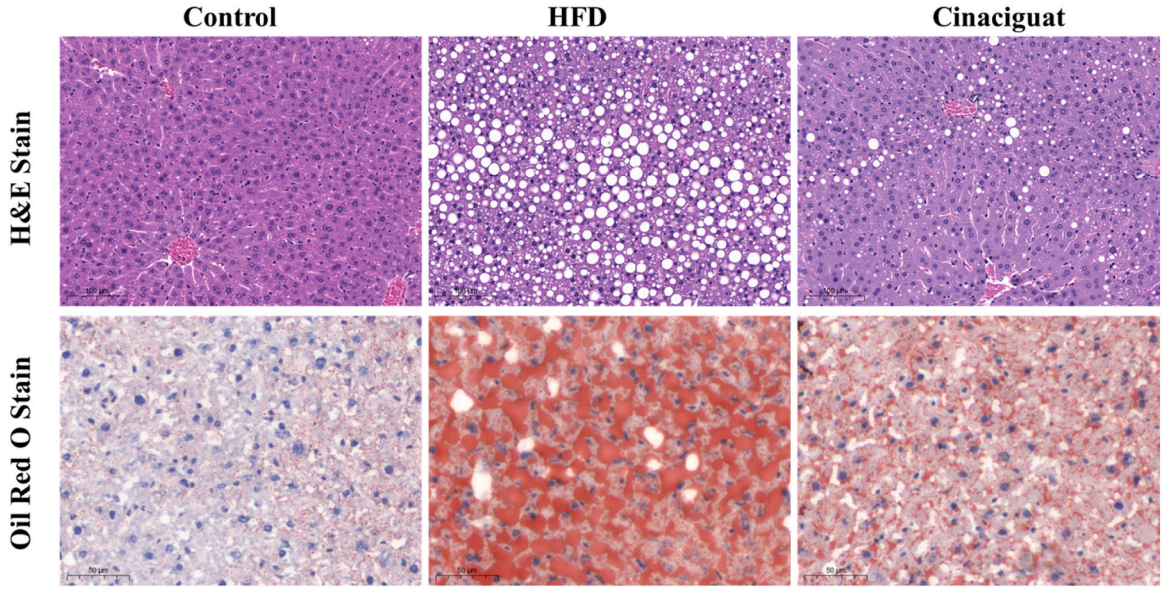

Fig. 8. Effect of cinaciguat on hepatic steatosis. Representative images of H&E and oil red-O stained liver tissue sections (Scale bar, 50 μm).

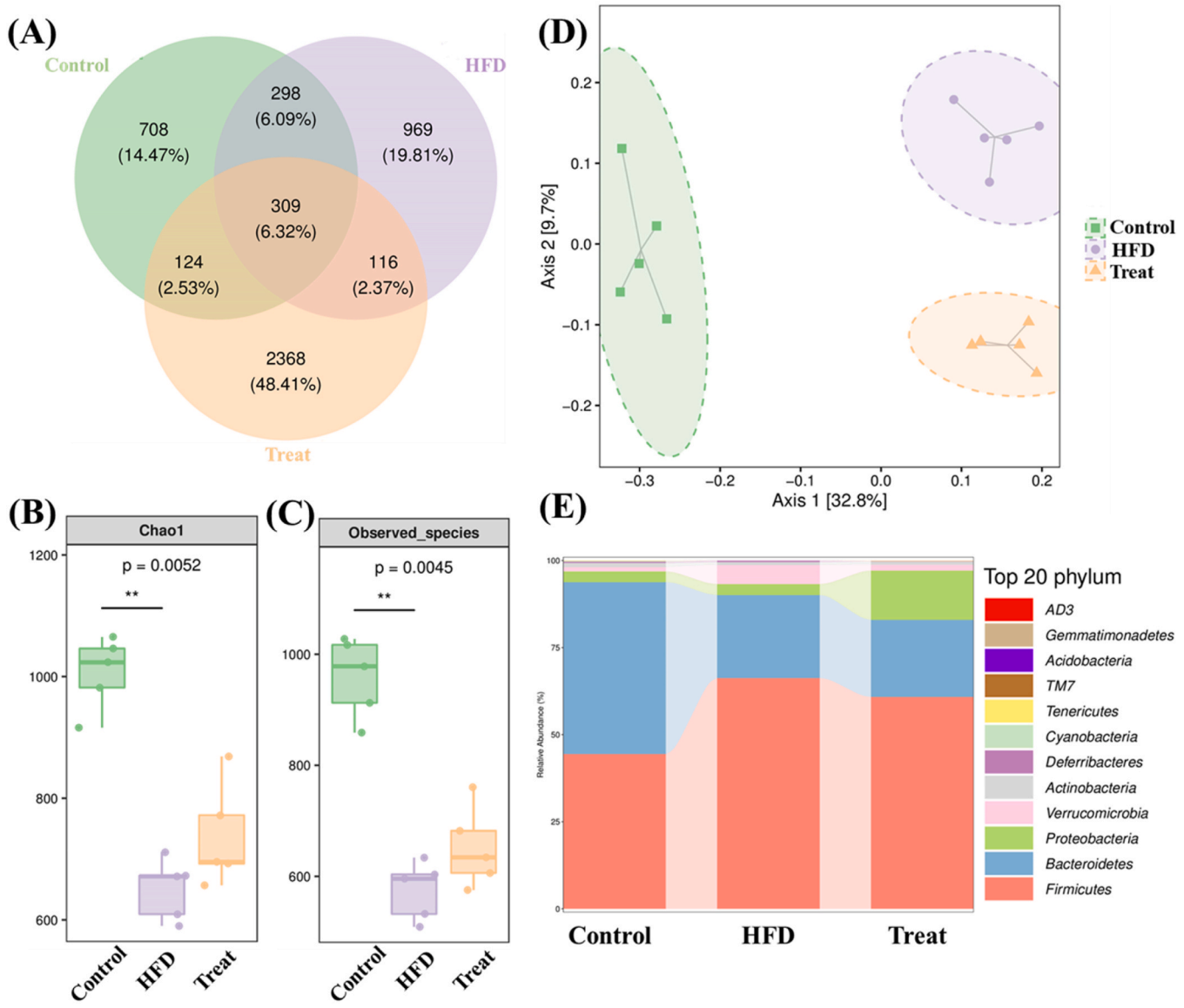

Fig. 9. Effect of cinaciguat treatment on the gut microbiota. (A) Venn diagrams of bacterial operational taxonomic units (OTUs). (B) Chao1 index of α-diversity. (C) Observed species index of α-diversity. (D) PCoA score plot based on unweighted UniFrac. (E) Phylum-level relative abundance of the gut microbiota.

(Fig. S8A). It was worth noted that *Desulfovibrionales* was considered to facilitate intestinal cholesterol absorption as suggested in a recent study, while *Desulfovibrionales* showed higher abundances in the cinaciguat treatment group, which may be due to the feedback regulation after cholesterol absorption was inhibited [35]. Moreover, the heat map and LEfSe analysis showed that HFD feeding decreased the relative abundance of *Alistipes*, which is consistent with previous research findings (Fig. S8B, S9) [22], while cinaciguat treatment slightly increased the abundance of *Alistipes* compared with the HFD group (Fig. S8B, S9). A negative correlation has been reported between *Alistipes* and obesity; thus, the increased abundance of *Alistipes* induced by cinaciguat may be beneficial for the reduction of triglycerides [36]. Furthermore, cinaciguat administration also increased the abundance of *Allobaculum* and *Roseburia* (Fig. S8B, S9). *Allobaculum* are associated with a higher plasma HDL concentration, and *Roseburia* has also received increasing attention due to its protective role in metabolic disorders such as atherosclerosis and obesity [37]. Taken together, these results suggested that HFD significantly altered the gut microbiome composition; however, cinaciguat treatment at least partly mitigated the HFD-induced microbiota dysbiosis.

3.8. Cinaciguat modulates the metabolome

Fluctuations in the composition of the gut microbiota lead to changes of gut microbiota–derived metabolites, which may play an important role in regulating the lipid metabolism of the host [19]. Untargeted metabolomics analysis of a feces sample was performed to assay the changes of metabolome. Both principal component analysis (PCA) and partial least squares discrimination analysis (PLS-DA) showed clear separation in the metabolic profiles among the three groups (Fig. 10 A, S10A). Volcano plot analyses were used to identify the unique metabolites, which suggested that 232 metabolites were significantly increased (red dots) in the HFD group compared with the Control group, and 210 metabolites were significantly decreased (blue dots) (Fig. S10B). In addition, the comparison between the Treat group and the HFD group revealed that 82 metabolites were more abundant in the Treat group (red dots), while 112 metabolites were less abundant (blue dots) (Fig. 10B). Venn diagrams of the significantly changed metabolites revealed that 21 metabolites in the Control group downregulated by HFD were reversed by cinaciguat treatment; further, 119 metabolites in the Control group upregulated by HFD were reversed by cinaciguat

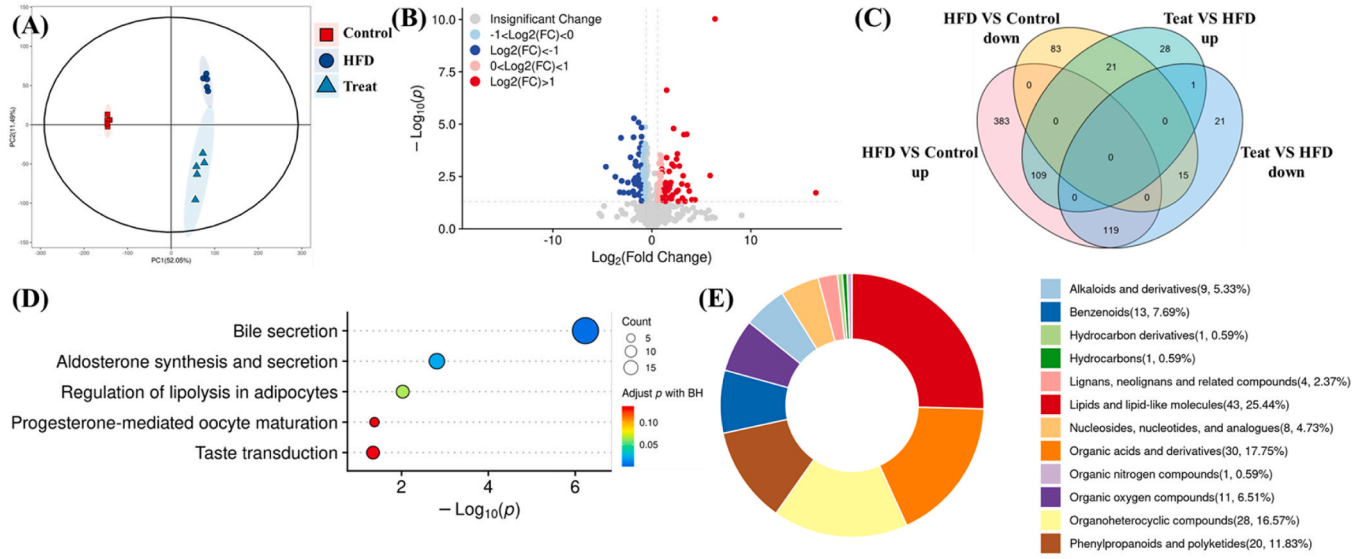

Fig. 10. (A) PCA score plot of the positive model. (B) Volcano plots of the Treat group vs. HFD group. (C) Venn analysis of significantly differential metabolites. (D) Enriched bubble map of the Treat group vs. HFD group in the mix model. (E) Diagram of the differential metabolite classification of the Treat group vs. HFD group in the mix model.

treatment (Fig. 10 C). Function analysis of the differential metabolites (top 30) in the Treat group and the HFD group showed that cinaciguat administration mainly regulated bile acid secretion metabolism (Fig. 10D). Moreover, according to the differential metabolite classification analysis between the Treat group and HFD group, lipids (25.44%) and organic acids (17.75%) were the main differential metabolites (Fig. 10E). It has been demonstrated that HFD significantly perturbs bile acid, which is closely related to hyperlipidemia [38,39]. Our findings indicated that the perturbation of bile acid levels induced by HFD was mitigated by cinaciguat treatment (Fig. S10C–E). Overall, our results demonstrated that cinaciguat significantly restored the HFD-induced metabolic changes. The effects of cinaciguat on metabolism may help to enhance its therapeutic efficiency on hyperlipidemia.

4. Discussion

Mixed hyperlipidemia, characterized by two different forms of lipid abnormalities (hypercholesterolemia and hypertriglyceridemia), is an important cause of cardiovascular diseases [40]. Representative drugs that are currently used in the clinical treatment of hyperlipidemia include 3-hydroxyl-3-methylglutaryl coenzyme A (HMG-CoA) reductase inhibitors, PCSK9 inhibitors, and NPC1L1 inhibitors [3]. However, these drugs do not reduce plasma levels of triglycerides and cholesterol at the same time. Therefore, the development of new bifunctional drugs for lowering both triglyceride and cholesterol levels is urgently needed. PTL and NPC1L1 have been identified as the key target proteins for intestinal absorption of triglycerides and cholesterol, respectively. Amal Kaddoumi et al. demonstrated that orlistat, a PTL inhibitor, could limit cholesterol intestinal absorption by inhibiting NPC1L1, which inspired us to design a bifunctional PTL/NPC1L1 inhibitor to simultaneously lower triglyceride and cholesterol levels [41]. To our knowledge, only one PTL/NPC1L1 dual inhibitor has been reported to date, and that one was designed by our team based on orlistat's structure [12]. However, the stability of this known inhibitor is not ideal, and in vivo activity remains unproven. Therefore, discovering new PTL/NPC1L1 dual inhibitors with higher potency and excellent drug properties is still needed, which could benefit patients with mixed hyperlipidemia.

To this end, we screened a series of small molecules targeting PTL and NPC1L1. Cinaciguat, a known agent used in the treatment of acute decompensated heart failure, displayed potent PTL-inhibition activity. Meanwhile, NBD-cholesterol and Filipin staining experiments demonstrated the excellent inhibition effect of cinaciguat against NPC1L1, which was comparable to that of ezetimibe. We simulated the interaction between cinaciguat and PTL (or NPC1L1) with docking software and found that the carboxyl group on the benzene ring played key roles in the binding models of PTL and NPC1L1. Subsequently, MD studies were used to confirm the stability of the interaction between cinaciguat and PTL (or NPC1L1). SPR analysis was employed to examine the affinity between cinaciguat and the two proteins. Moreover, a kinetic study revealed a competitive inhibition profile of cinaciguat for PTL and NPC1L1. However, although cinaciguat was obtained through virtual screening based on the catalytic active site of PTL and the cholesterol-binding site of NPC1L1, and the interactions between cinaciguat and PTL (or NPC1L1) proteins were determined using multiple approaches, without cocrystal structure evidence it is difficult to identify the direct binding sites of cinaciguat within PTL and NPC1L1 proteins. Further structural biology studies should reveal more information on the effects of cinaciguat on PTL and NPC1L1.

Next, we evaluated the lipid-lowering effects of cinaciguat in a mouse model. Cinaciguat significantly reduced body weight and the levels of triglycerides, total cholesterol, and LDL-C, meanwhile increase of HDL-C level. In addition, the expression level of NPC1L1 in the small intestine was significantly inhibited by cinaciguat according to western blot findings. Furthermore, HFD-induced lipid vacuoles and lipid droplet accumulation in the liver was significantly attenuated by cinaciguat according to H&E and oil red-O staining analyses. Further, we found that cinaciguat mitigated the HFD-induced microbiota dysbiosis and restored HFD-induced metabolic changes. In addition to the effects of intestinal absorption of triglycerides and cholesterol mediated by PTL and NPC1L1 on lipid levels, multiple target proteins (e.g., HMG-CoA and PCSK9) affect lipid levels [42–44]. Additional mechanisms of cinaciguat effects on other proteins involved in the regulation of lipid metabolism are our future interests.

5. Conclusions

In summary, the present study demonstrated that cinaciguat, a novel PTL/NPC1L1 dual inhibitor, effectively inhibited the uptake of triglycerides and cholesterol, and it showed potent lipid-lowering activity in an HFD-induced mixed hyperlipidemia model. The pharmacological mechanisms were assessed in multiple ways. Cinaciguat is a potential candidate molecule worthy of further development for clinical

application in the treatment of mixed hyperlipidemia.

CRediT authorship contribution statement

Ang Jia: Formal analysis, Data curation, Project administration. **Hongfei Jiang:** Software, validation, visualization. **Wenjing Liu:** Formal analysis, data curation. **Pengwei Chen:** Data curation, Writing – original draft, Writing - review & editing. **Renshuai Zhang:** Resources, Writing – review & editing, validation, supervision. **Qi Xu:** Resources, supervision, writing - review & editing. **Jufeng Sun:** Conceptualization, Methodology, Writing – review & editing.

Declaration of Competing Interest

The authors declare that they have no known competing financial interests or personal relationships that could have appeared to influence the work reported in this paper.

Data Availability

Data will be made available on request.

Acknowledgements

We thank Shanghai Bioprofile Technology Co., Ltd. for technical support. We appreciated the compound library from Targetmol, USA. Thanks to Dr. Gang Li and Xiaoping Peng for providing the small molecule natural products, which increased the variety of compounds we screened. We are grateful to the Natural Science Foundation of Hainan Province (220RC703), Natural Science Foundation of Shandong Province (ZR2022QH051, ZR2021QH212, ZR2020QC081), Science, Education and Industry Integration Innovation Pilot Project from Qilu University of Technology (Shandong Academy of Sciences) (2022JBZ02-04) for financial support.

Author contributions

RSZ and JFS designed the research. AJ, HFJ, WJL, and QX conducted experiments and acquired the data. AJ, HFJ, WJL, PWC, QX, RSZ and JFS performed data analysis. QX, RSZ, PWC and JFS wrote and revised the manuscript.

Appendix A. Supporting information

Supplementary data associated with this article can be found in the online version at doi:10.1016/j.phrs.2023.106854.

References

[1] Arupkr Malakar, Debashree Choudhury, Binata Halder, Prosenjit Paul, Arif Uddin, Supriyo Chakraborty. A review on coronary artery disease, its risk factors, and therapeutics, J. Cell. Physiol. 234 (2019) 16812–16823.
[2] Kaushik Biswas, Ajoy Tiwari, Prachi Jadhav, Amit Goel, Gv Chanukya. Rosuvastatin and fenofibrate combination in the treatment of mixed hyperlipidemia: a narrative review, J. Curr. Med. Res. Opin. 4 (2021) 867–877.
[3] Qian Xu, Yiming Deng, Jun Xiao, Xiangrui Liu, Min Zhou, Zhong Ren, Juan Peng, Yaling Tang, Zhisheng Jiang, Zhihan Tang, Lushan Liu, Three musketeers for lowering cholesterol: statins, ezetimibe and evolocumab, Curr. Med. Chem. 28 (2021) 1025–1041.
[4] Jonas Hallén, Nadarajah Sreeharan, Development of triglyceride-lowering drugs to address residual cardiovascular risk: strategic and clinical considerations, Eur. Heart J. Cardiavasc. Pharmacother. 4 (2018) 237–242.
[5] Adelhajj Ali, Nour Younis, Rola Abdallah, Farah Shaer, Ali Dakroub, Mohammedakli Ayoub, Rabah Iratni, Hadimohamad Yassine, Kazem Zibara, Alexander Orekhov, Ahmedfawzy El-Yazbi, Alih Eid, Lipid-lowering therapies for atherosclerosis: statins, fibrates, ezetimibe and pcsk9 monoclonal antibodies, Curr. Med. Chem. 28 (2021) 7427–7445.
[6] Rahulb Birari, Kamleshk Bhutani, Pancreatic lipase inhibitors from natural sources: unexplored potential, Drug Discov. Today 12 (2007) 879–889.
[7] Scottw Altmann, Harryr Davis, Luquan Wang, Nicholas Murgolo, Michaelp Graziano, Li-ji Zhu, Xiaorui Yao, Lizbethm Hoos, Glen Tetzloff, Saiprasadn Iyer, Niemann-pick c1 like 1 protein is critical for intestinal cholesterol absorption, Science 303 (2004) 1201–1204.
[8] Yuguang Shi, Paul Burn, Lipid metabolic enzymes: emerging drug targets for the treatment of obesity, Nat. Rev. Drug Discov. 3 (2004) 695–710.
[9] Chuhan Fu, Yao Jiang, Jiao Guo, Zhengquan Su, Natural products with anti-obesity effects and different mechanisms of action, J. Agric. Food Chem. 64 (2016) 9571–9585.
[10] Lin Jia, Niemann-pick c1-like 1 (npc1l1) protein in intestinal and hepatic cholesterol transport, Annu. Rev. Physiol. 73 (2011) 239–259.
[11] Renshuai Zhang, Wenjing Liu, Jun Zeng, Jingsen Meng, Hongfei Jiang, Jie Wang, Dongming Xing, Niemann-pick c1-like 1 inhibitors for reducing cholesterol absorption, Eur. J. Med. Chem. 230 (2022), 114111.
[12] Renshuai Zhang, Zhengming Song, Xueting Wang, Jiao Xue, Dongming Xing, One-step modification to identify dual-inhibitors targeting both pancreatic triglyceride lipase and niemann-pick c1-like 1, Eur. J. Med. Chem. 216 (2021), 113358.
[13] Niteshmani Tripathi, Anupam Bandyopadhyay, High throughput virtual screening (htvs) of peptide library: technological advancement in ligand discovery, Eur. J. Med. Chem. 243 (2022), 114766.
[14] Mp Egloff, F. Marguet, G. Buono, R. Verger, C. Cambillau, H. van Tilbeurgh, The 2.46 a resolution structure of the pancreatic lipase-colipase complex inhibited by a c11 alkyl phosphonate, Biochemistry 34 (1995) 2751–2762.
[15] Ching-shin Huang, Xinchao Yu, Preston Fordstrom, Kaylee Choi, Benc Chung, Soung-hun Roh, Wah Chiu, Mingyue Zhou, Xiaoshan Min, Zhulun Wang, Menloparkcaunited Slac National Accelerator Lab. Cryo-em structures of npc1l1 reveal mechanisms of cholesterol transport and ezetimibe inhibition, Sci. Adv. 6 (2020) 1989.
[16] Miaoqing Hu, Fan Yang, Yawen Huang, Xin You, Desheng Liu, Shan Sun, Sen-fang Sui, Structural insights into the mechanism of human npc1l1-mediated cholesterol uptake, Sci. Adv. 7 (2021) 3188.
[17] Tao Long, Yang Liu, Yu Qin, Russella Debose-Boyd, Xiaochun Li, Structures of dimeric human npc1l1 provide insight into mechanisms for cholesterol absorption, Sci. Adv. 7 (2021) 3997.
[18] W. Jia, G. Xie, W Jia. Bile acid-microbiota crosstalk in gastrointestinal inflammation and carcinogenesis, Nat. Rev. Gastroenterol. Hepatol. 15 (2018) 111–128.
[19] Allison Agus, Karine Clément, Harry Sokol, Gut microbiota-derived metabolites as central regulators in metabolic disorders, Gut 70 (2021) 1174–1182.
[20] Sisi Yan, Jihong Chen, Lingfeng Zhu, Tianyi Guo, Dandan Qin, Zuomin Hu, Shuai Han, Ji Wang, Froilanbernard Matias, Lixin Wen, Feijun Luo, Qinlu Lin, Oryzanol alleviates high fat and cholesterol diet-induced hypercholesterolemia associated with the modulation of the gut microbiota in hamsters, Food Funct. 13 (2022) 4486–4501.
[21] Jiaojiao Gu, Lulu Jing, Xiaotao Ma, Zhaofeng Zhang, Qianying Guo, Yong Li, Gc–tof-ms-based serum metabolomic investigations of naked oat bran supplementation in high-fat-diet-induced dyslipidemic rats, J. Nutr. Biochem. 26 (2015) 1509–1519.
[22] Jiangmin Fang, Lirong Zeng, Yalun He, Xiong Liu, Tongcun Zhang, Qiong Wang, Effects of dietary tannic acid on obesity and gut microbiota in c57bl/6j mice fed with high-fat diet, Foods 11 (2022) 3325.
[23] Yaqing Chang, Dan Zhang, Guiya Yang, Yuguang Zheng, Long Guo, Screening of anti-lipase components of artemisia argyi leaves based on spectrum-effect relationships and hplc-ms/ms, Front. Pharmacol. 12 (2021).
[24] Wenjing Liu, Bing Liang, Jun Zeng, Jingsen Meng, Lingyu Shi, Shanbo Yang, Jing Chang, Chao Wang, Xiaokun Hu, Xufu Wang, Na Han, Chenghui Lu, Jiao Li, Congcong Wang, Huanting Li, Renshuai Zhang, Dongming Xing, First discovery of cholesterol-lowering activity of parthenolide as npc1l1 inhibitor, Molecules 27 (2022) 6270.
[25] Qi Xu, Renshuai Zhang, Yan Mu, Yue Song, Na Hao, Yunbo Wei, Quanbo Wang, Charlesr Mackay, Propionate ameliorates alcohol-induced liver injury in mice via the gut–liver axis: focus on the improvement of intestinal permeability, J. Agric. Food Chem. 70 (2022) 6084–6096.
[26] Jingsen Meng, Jiazhen Xu, Shanbo Yang, Wenjing Liu, Jun Zeng, Lingyu Shi, Jing Chang, Renshuai Zhang, Dongming Xing, Emodin lows npc1l1-mediated cholesterol absorption as an uncompetitive inhibitor, Bioorg. Med. Chem. Lett. (2022), 128974.
[27] Jun Zeng, Wenjing Liu, Bing Liang, Lingyu Shi, Shanbo Yang, Jingsen Meng, Jing Chang, Xiaokun Hu, Renshuai Zhang, Dongming Xing, Inhibitory effect of isoliquiritigenin in niemann-pick c1-like 1-mediated cholesterol uptake, Molecules 27 (2022) 7494.
[28] Chen-chen Gu, Jun Zeng, Xiao-ping Peng, Yan-jun Sun, Shuang-zhi Yuan, Xiu-ning Wang, Ren-shuai Zhang, Hong-xiang Lou, Gang Li, Cytochalasans with inhibitory activity against npc1l1 from the endophytic fungus chaetomium nigricolor f5, J. Org. Chem. 88 (2023) 3185–3192.
[29] Qing Hu, Xiao-qing Guan, Li-lin Song, Hao-nan Wang, Yuan Xiong, Jun-ling Liu, Heng Yin, Yun-feng Cao, Jie Hou, Ling Yang, Guang-bo Ge, Inhibition of pancreatic lipase by environmental xenoestrogens, Ecotoxicol. Environ. Saf. 192 (2020), 110305.
[30] C. Bt Nemeth, A. Matyas, A. Olah, L. Lux, M. Hidi, D. Ruppert, G. Kellermayer, G. Kokeny, B. Szabo, Merkely, T Radovits. Cinaciguat prevents the development of pathologic hypertrophy in a rat model of left ventricular pressure overload, Sci. Rep. 6 (2016) 37166.
[31] S. Czirok, L. Fang, T. Radovits, G. Szabo, G. Szenasi, L. Rosivall, B. Merkely, G. Kokeny, Cinaciguat ameliorates glomerular damage by reducing erk1/2 activity and tgf-ss expression in type-1 diabetic rats, Sci. Rep. 7 (2017) 11218.

[32] J. Joshua, Gk Schwaerzer, H. Kalyanaraman, E. Cory, Rl Sah, M. Li, F. Vaida, Gr Boss, Rb Pilz, Soluble guanylate cyclase as a novel treatment target for osteoporosis, Endocrinology 155 (2014) 4720–4730.
[33] Qi Zhao. Preventive effect of soluble guanglate cyclase activator cinaciguat in diabetes macrovasculopathy. Shandong University (Thesis for master degree). 2016.
[34] Liang Ge, Jing Wang, Wei Qi, Hong-hua Miao, Jian Cao, Yu-xiu Qu, Bo-liang Li, Bao-liang Song, The cholesterol absorption inhibitor ezetimibe acts by blocking the sterol-induced internalization of npc1l1, Cell Metab. 7 (2008) 508–519.
[35] Hai Hu, Wentao Shao, Qian Liu, Ning Liu, Qihan Wang, Jin Xu, Xin Zhang, Zhenkun Weng, Qifan Lu, Long Jiao, Chaobo Chen, Haidong Sun, Zhaoyan Jiang, Xiaoping Zhang, Aihua Gu, Gut microbiota promotes cholesterol gallstone formation by modulating bile acid composition and biliary cholesterol secretion, Nat. Commun. 13 (2022) 252.
[36] Yajian Song, Huitao Shen, Tingting Liu, Bingju Pan, Sanduni De Alwis, Wanyi Zhang, Xuegang Luo, Zhongyuan Li, Nan Wang, Wenjian Ma, Tongcun Zhang, Effects of three different mannans on obesity and gut microbiota in high-fat diet-fed c57bl/6j mice, Food Funct. 12 (2021) 4606–4620.
[37] Man Zhang, Xin Zhang, Jieyu Zhu, Denggao Zhao, Yanyan Ma, Dongli Li, Chitang Ho, Qingrong Huang, Bidirectional interaction of nobiletin and gut microbiota in mice fed with a high-fat diet, Food Funct. 12 (2021) 3516–3526.
[38] Huijuang Ma, Maryelizabeth Patti, Bile acids, obesity, and the metabolic syndrome, Best. Pract. Res. Clin. Gastroenterol. 28 (2014) 573–583.
[39] Tung-ting Sham, Meng-heng Li, Chi-on Chan, Huan Zhang, Shun-wan Chan, Danielkam-wah Mok, Cholesterol-lowering effects of piceatannol, a stilbene from wine, using untargeted metabolomics, J. Funct. Foods 28 (2017) 127–137.
[40] Eskandar Taghizadeh, Rezajafarzadeh Esfehani, Amirhossein Sahebkar, Seyedmostafa Parizadeh, Daryoush Rostami, Mohammadreza Mirinezhad, Arash Poursheikhani, Majidghayour Mobarhan, Alireza Pasdar, Familial combined hyperlipidemia: an overview of the underlying molecular mechanisms and therapeutic strategies, Iubmb Life 71 (2019) 1221–1229.
[41] Saeed Alqahtani, Hisham Qosa, Brian Primeaux, Amal Kaddoumi, Orlistat limits cholesterol intestinal absorption by niemann-pick c1-like 1 (npc1l1) inhibition, Eur. J. Pharmacol. 762 (2015) 263–269.
[42] Be Haines, O. Wiest, Cv Stauffacher, The increasingly complex mechanism of hmg-coa reductase, Acc. Chem. Res. 46 (2013) 2416–2426.
[43] Qm Melendez, St Krishnaji, Cj Wooten, D. Lopez, Hypercholesterolemia: the role of pcsk9, Arch. Biochem. Biophys. 625- 626 (2017) 39–53.
[44] Ningning Ma, Lei Fan, Yunxia Dong, Xiaoding Xu, Chuwei Yu, Jing Chen, Jin Ren, New pcsk9 inhibitor mir-552-3p reduces ldl-c via enhancing ldlr in high fat diet-fed mice, Pharmacol. Res. 167 (2021), 105562.